NeuroImage 193 (2019) 201–213

Contents lists available at ScienceDirect

NeuroImage

journal homepage: www.elsevier.com/locate/neuroimage

Distinct modes of top-down cognitive processing in the ventral visual cortex

Han-Gue Jo [a], Thilo Kellermann [a,b], Conrad Baumann [c], Junji Ito [b,d], Barbara Schulte Holthausen [a], Frank Schneider [a,f], Sonja Grün [b,d,e], Ute Habel [a,b,*]

[a] Department of Psychiatry, Psychotherapy and Psychosomatics, Medical Faculty, RWTH Aachen University, 52074, Aachen, Germany
[b] JARA-Institute Brain Structure Function Relationship (INM-10), Research Center Jülich and RWTH Aachen University, 52074, Aachen, Germany
[c] Median Klinik Mecklenburg, 19217, Rehna, Germany
[d] Institute of Neuroscience and Medicine (INM-6) and Institute for Advanced Simulation (IAS-6), Research Center Jülich, 52425, Jülich, Germany
[e] Theoretical Systems Neurobiology, Faculty I, RWTH Aachen University, 52056, Aachen, Germany
[f] University Hospital, Heinrich-Heine-University of Duesseldorf, 40225 Duesseldorf, Germany

ARTICLE INFO

Keywords:
Top-down
Cognitive processing
Eye-movement
EEG
DCM

ABSTRACT

Top-down cognitive control leads to changes in the sensory processing of the brain. In visual perception such changes can take place in the ventral visual cortex altering the functional asymmetry in forward and backward connections. Here we used fixation-related evoked responses of EEG measurement and dynamic causal modeling to examine hierarchical forward-backward asymmetry, while twenty-six healthy adults performed cognitive tasks that require different types of top-down cognitive control (memorizing or searching visual objects embedded in a natural scene image). The generative model revealed an enhanced asymmetry toward forward connections during memorizing, whereas enhanced backward connections were found during searching. This task-dependent modulation of forward and backward connections suggests two distinct modes of top-down cognitive processing in cortical networks. The alteration in forward-backward asymmetry might underlie the functional role in the cognitive control of visual information processing.

1. Introduction

Visual information of an object passes a series of processing levels in a hierarchy from the early visual areas to the anterior inferotemporal cortex (IT), the ventral visual pathway (Goodale and Milner, 1992). The visual features are processed progressively across the hierarchy from the analysis of simple visual features in the lower-order areas (V1, V2) to complex object representations in the higher-order areas (V4, IT). However, studies revealed that the ventral pathway is not a unidirectional network, but it possesses both ascending forward and descending backward connections (Felleman and Van Essen, 1991; Pollen, 1999). While forward connections enable bottom-up processing of the external sensory inputs, backward connections carry information that provides contextual guidance from higher levels to the lower-order areas to facilitate task-relevant processing of the sensory inputs (Gilbert and Li, 2013), referred to as top-down processing. Therefore, in situations where different types of such top-down processing are required, it is expected that forward and backward connections would be differentially employed according to the context.

Recent evidence denotes the electrophysiological response following eye fixation (fixation-related evoked potential, FRP) as a neural marker of natural visual processing (Nikolaev et al., 2016; Ossandón et al., 2010). Such FRP approach allows investigating neural activities underlying unconstrained voluntary eye-movements, which resemble natural visual exploration. FRP has been associated with cognitive processes of identification and recognition of objects during visual search (Kamienkowski et al., 2012; Kaunitz et al., 2014), suggesting that the generation of the FRP not only relies on bottom-up sensory processing but also reflects top-down cognitive processing. Indeed, it has been demonstrated that evoked responses are generated by forward and backward connections in cortical networks (Garrido et al., 2007). These raise the question of how the forward and backward connections contribute to the generation of FRP when top-down processing guides task-dependent visual processes.

To answer this question, we acquired electroencephalography (EEG) activity following each eye fixation as part of a simultaneous EEG-fMRI measurement. Subjects performed different task conditions while viewing a complex natural scene image: searching for a target object, memorizing objects, or freely viewing such a complex image (Fig. 1A). We hypothesized that cognitive load in the memorizing and searching

* Corresponding author. Department of Psychiatry, Psychotherapy and Psychosomatics, Medical Faculty, RWTH Aachen University, 52074, Aachen, Germany.
E-mail address: uhabel@ukaachen.de (U. Habel).

https://doi.org/10.1016/j.neuroimage.2019.02.068
Received 2 August 2018; Received in revised form 11 January 2019; Accepted 27 February 2019
Available online 5 March 2019
1053-8119/

tasks would lead to greater modulatory effects on the forward or backward interactions within the cortical areas that are associated with identification as well as recognition of visual objects (Goodale and Milner, 1992), than a mere free viewing of equivalent images. In order to assess the forward and backward connection strengths underlying the measured cortical responses, we employed dynamic causal modeling (DCM; David et al., 2006), which rests on the generative model of visual evoked potential (Jansen and Rit, 1995) and the connection rules among cortical sources in the visual cortex (Felleman and Van Essen, 1991).

2. Materials and methods

2.1. Participants

Thirty-two young healthy volunteers (under/graduate students) took part in the study. Hand preference was assessed with a German version of handedness questionnaire (the Edinburgh inventory; Oldfield, 1971) and all subjects were right-handed. They had normal or corrected-to-normal visual acuity and were free from any history of neurological or psychiatric diseases. Written informed consent was collected from each subject

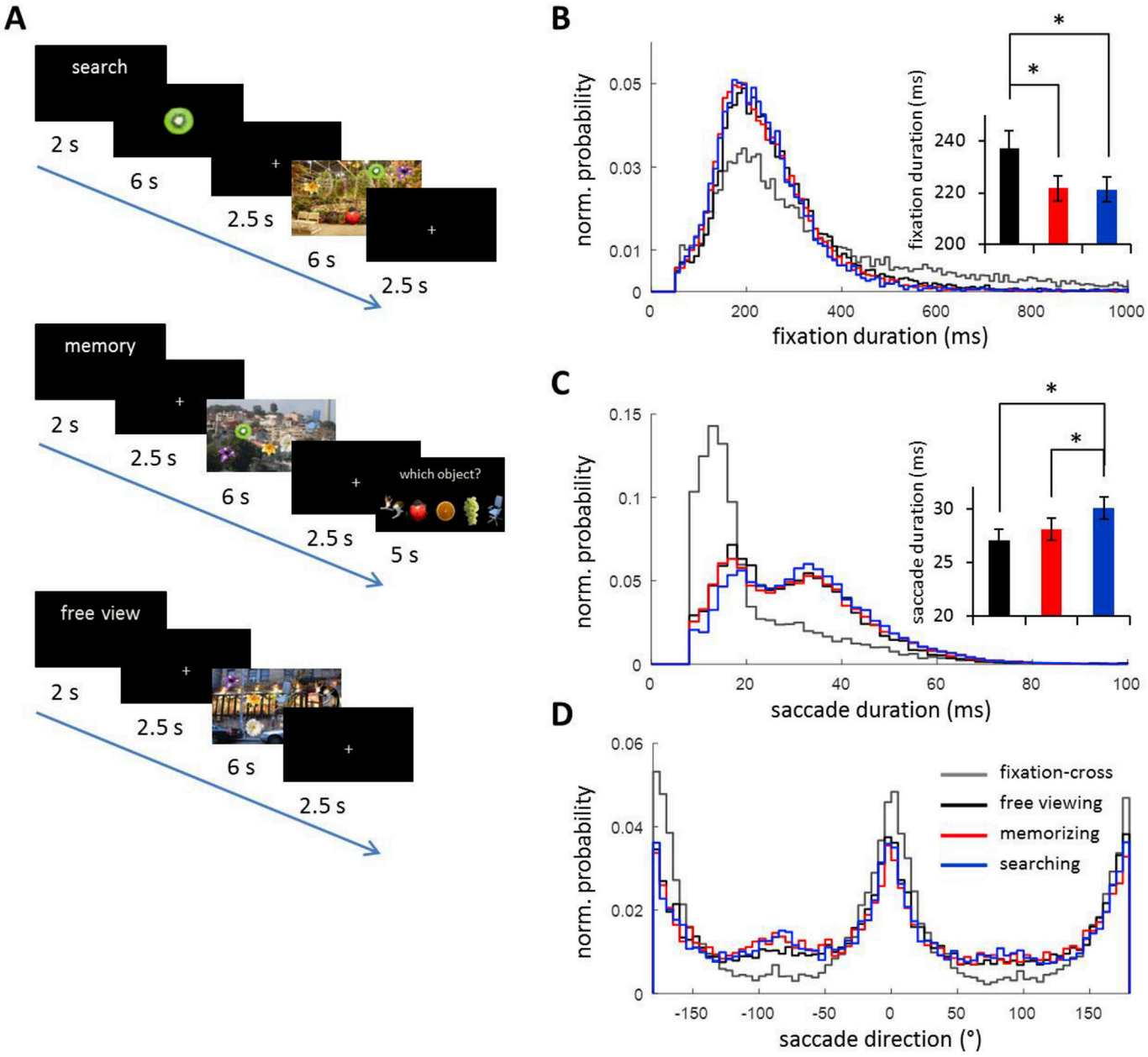

Fig. 1. Sequence of events in each task condition and eye-movement characteristics. (A) The time course of each condition is shown in seconds. Eye-movements and fixation-related brain responses were extracted during the 6-s presentations of natural scene images of each task condition (i.e., 30 trials for each searching, memorizing, and free viewing conditions) and fixation-cross presentation. For searching condition, subjects were required to search the scene for a target object, while during memorizing condition they memorized all objects embedded in the scene. No specific instruction was given for the free viewing condition (for details see Method section). Note that the objects embedded in natural scene images are stretched and randomly located for illustration purpose. The objects consisted of flowers, animals, insects, fruits, furniture, tools, and transports (Supplementary Fig. 1). Normalized probabilities of fixation (B) and saccade (C) durations across all subjects are shown in 2 ms bin histograms. Insert panels depict the mean eye-movement durations for each task condition. Error bars represent standard error of the mean. *, corrected $p < 0.05$. (D) Illustrates saccade directions in a 5° bin histogram across all subjects. Directions near to 0 and ±180° indicate horizontal movements, whereas near to ±90° indicate vertical movements.

after the procedure was fully explained. The study was approved by the ethics committee of RWTH Aachen University Hospital. Data of six subjects were discarded from the analysis due to artifacts and technical failure during recordings. As a result, twenty-six subjects (ages 19–29, 12 females) were included in the present analysis.

2.2. Task protocol

Subjects performed voluntary visual exploration of natural scene images under three different task conditions: searching cognitive-task, memorizing cognitive-task, and free viewing non-cognitive-task (Fig. 1A). Each subject performed 30 trials for each task condition, resulting in a total of 90 trials per subject. Trials of the three different conditions were pseudo-randomly distributed among the 90 trials, avoiding the same condition three times in a row. Each trial began with a 2 s display of a task indicator, which is German words written in white against black background: 'SUCHE das folgende Objekt!' (SEARCH for the following object) for the searching condition, 'MERKE Dir die Objekte im folgenden Bild!' (MEMORIZE the objects in the following image) for the memorizing condition, or 'SCHAUE Dir das folgende Bild nur an!' (merely LOOK at the following image) for the free viewing condition. Following the instruction, for the searching condition, a target object was first displayed for 6 s and then a scene image was presented for 6 s, during which subjects had to search the scene for the target object (every scene image contained 5 different objects; see "Stimulus preparation and presentation" below) and had to press the middle button of a three-response button device as soon as they found the object. In contrast, for the memorizing condition, a scene image was first presented for 6 s after the task indicator and subjects were required to find and memorize all five objects in the scene. Afterwards, they were presented with a probe array consisting of five objects with a cursor over one of them, among which only one object had been present in the scene image. Subjects were given 5 s for a response by pressing the left and right buttons for moving the cursor to the left and right, respectively, and pressing the middle button for selection. For the free viewing condition, a scene image was presented for 6 s after the task indicator and subjects viewed the scene freely without any requested cognitive task. In all three conditions, a white central fixation-cross was presented for 2.5 s before and after the scene presentation. The same fixation-cross was also presented for a random interval of 5.5–8 s between the trials. Subjects were instructed to maintain fixation on the cross during stimulus presentation.

2.3. Stimulus preparation and presentation

The scene image stimuli for the three task conditions were generated by placing object images on background images of natural scenes. For the objects, we drew 39 object images from the Microsoft image gallery (Supplementary Fig. 1) and resized them (keeping the aspect ratios) to a size of 143.56 ($\pm$6.7 standard-error of the mean (SEM)) $\times$ 141.10 ($\pm$3.5 SEM) pixels on average. For the background, we collected 15 natural scene images of 1920 $\times$ 1200 pixels, 8 of which were pictures taken by one of the coauthors and the rest were taken from the Internet. The images were photos of plants, flowers, fruits, gardens, boats, rooms, streets, and churches (not shown here for copyright reasons; details are available on request to the authors). To find positions to place an object in a given background such that the object would naturally blend into the background, we computed a contrast map for every pair of object and background images in the following manner: 1) place the object at a starting position (e.g., upper left) on the background image, 2) compute the hue, saturation and luminance contrasts between each pixel of the object image and the pixel of the occluded background image at the corresponding position, 3) derive a contrast index for the present position by averaging the obtained contrast values across the pixels and the properties (i.e., hue, saturation and luminance), and 4) repeat this procedure for every position within the background to yield a map of the contrast index values. Based on such a contrast map, three candidate positions for the placement of the object were identified as the positions of the three lowest contrast index values in the contrast map for each pair of an object and a background. To generate stimulus images, we selected two sets of 5 objects for each background image, such that the candidate placing positions of the objects within a set do not overlap with each other. We generated 3 stimulus images using one set of 5 objects for a given background by overlaying the object images on the background image at their candidate placing positions. Thus, a total of 90 stimulus images were generated based on 30 combinations of 15 backgrounds x 2 sets of 5 objects; each combination served for 3 variants of a stimulus image which differed only in the object positions. We used each of the three variants in each of the three task conditions, assuring that each and every combination appeared only once in each task condition.

The presentation of the images (background plus 5 placed objects) for each trial was implemented using the Presentation software (Neurobehavioral Systems, USA). The images were presented on a monitor screen (BOLDscreen, Cambridge Research Systems Ltd) at a refresh rate of 60 Hz and they were mirrored to redirect the subject's line of sight during MRI measurement. The scene images were displayed with a 1920 $\times$ 1200 pixels resolution, subtending 25.4 $\times$ 16.0° of visual angle.

2.4. Data acquisition

Participants were placed in a 3 T MR scanner (Siemens MAGNETOM Prisma®, Siemens Medical Systems, Germany) with their right fingers positioned on a three-response button device. Before the main task, a 4 min magnetization-prepared rapid acquisition gradient echo image (MPRAGE) T1-weighted sequence was used to acquire structural images (TR = 1900 ms, TE = 2.52 ms, matrix = 256 $\times$ 256, 176 slices, voxel size = 1 $\times$ 1 $\times$ 1 mm^3, flip-angle 9°). During the main task, functional imaging was performed using echo-planar imaging sensitive to BOLD contrast (voxel size: 3.0 $\times$ 3.0 $\times$ 3.0 mm^3, 64 $\times$ 64 matrix, 36 slices, TR 1950 ms, TE 30 ms, flip-angle 76°), but this data was not used in the present study. An MR-compatible EEG amplifier system (two BrainAmp MR plus 32-channel amplifiers, Brain Products, Germany) and a sync box (Brain Products) were used for synchronization of the EEG recordings with the MRI slice acquisition. EEG data were recorded in BrainVision Recorder software (v 1.05, Brain Products) at a sampling rate of 5000 Hz using an analog band-pass filter between 0.01 Hz and 250 Hz. An additional ECG electrode was placed under the left collar bone. AFz and FCz served as the recording reference and ground, respectively. EEG impedance levels were kept below 10 kΩ. Eye-movements were recorded from the right eye with an EyeLink 1000 Plus system (SR Research, Canada) at a sampling rate of 1000 Hz. The EEG and eye tracking recordings were synchronized by triggers that occurred at the onset of each event (i.e., task instruction, object, scene image and fixation-cross stimuli; Fig. 1A). MR gradient artifacts in the EEG signal were removed using the average artifact subtraction method (Allen et al., 2000) as implemented in the Brain Vision Analyzer 2.0 (Brain Products), in which a template of the MR artifact was constructed with a sliding average of 25 volumes. Subsequently, the EEG data were corrected for the ballistocardiogram artifacts using a semi-automatic pulse detection method of the ECG channel and a template averaging method (Allen et al., 1998). The averaged pulse waveform aligned to an ECG episode was subtracted from the EEG data for each ECG episode as implemented in the Brain Vision Analyzer 2.0.

2.5. EEG and eye-movement analysis

The analysis of the EEG data and the eye-movements was performed using EEGLAB (Delorme and Makeig, 2004), its extension EYE-EEG (Dimigen et al., 2011), and SPM12 (Litvak et al., 2011) for integrated analyses. Saccades were detected as outliers in 2D velocity space introduced by Engbert and Mergenthaler (2006); velocity threshold = 5 SD). Additionally, saccades were required to last 6 ms or more, but less than 100 ms. Saccades occurring within 100 ms before and after an eye-blink were removed. Fixations were defined starting at the saccade offset. Only

fixations located on the screen with a minimum duration of 50 ms were included in the analysis. The median value of individual saccade and fixation durations that survived after EEG artifact correction (see below) was subjected to a repeated measures ANOVA with the task condition as a within-subject factor. The Greenhouse-Geisser correction was used to estimate epsilon (ε) when the assumption of sphericity of repeated-measures ANOVAs was violated.

The MRI artifact-removed EEG data were filtered with a high-pass filter at 0.1 Hz, using Hamming windowed FIR filter, and down sampled to 500 Hz. Few poor contact electrodes of individual measurements were screened by visual inspection and were replaced through spherical interpolation (on average 1.7 ± 0.2 electrodes per subject). Independent component analysis (ICA) was performed and the components, representing residuals of the ballistocardiogram and the ocular movements mainly over the frontal areas, were identified and removed. The continuous EEG recording was then segmented from −100 to 200 ms time-locked to the fixation onset that occurred during scene presentation. We considered an individual sequence of a saccade and the following fixation as one 'trial', and aligned the signals on the fixation onset times. Baseline correction was applied by subtracting the mean voltage at 100 ms prior to the fixation onset. Note, however, that selection of a baseline interval is a challenge in EEG-eye movement analysis (Nikolaev et al., 2016). Although saccade-related distortion of the baseline activity might compound with effects of task conditions, matching the saccade duration showed the same pattern of baseline activity between task conditions (see *Neural correlates of task conditions* in the Results and Supplementary Fig. 2). For the searching condition, fixation segments that occurred after the button press were excluded from the analysis to ensure the context of the searching condition. We also randomly sampled 400 fixation-locked segments of each subject during the presentations of the fixation-cross (fixation-cross condition) that were presented between task conditions. Segments from all conditions were visually inspected offline, and those containing muscular activities or non-physiological artifacts were rejected. On average, 372.3 (±11.5 SEM), 410.7 (±18.2 SEM), 479.5 (±17.0 SEM), 355.4 (±12.2 SEM) segments per subject were analyzed for the fixation-cross, free viewing, memorizing and searching conditions, respectively. Fixation-related potentials (FRPs; Fig. 2) were then obtained for each subject by averaging the segments for each condition.

For sensor space analyses, EEG segments (before averaging for each condition) were transformed to scalp current density (SCD; Kayser and Tenke, 2006), which emphasizes local electrical activity and reduces volume conduction effects of surface EEG recordings. The constant transformation parameters were set to the default values (spherical spline flexibility $m = 4$, smoothing constant $\lambda = 10^{-5}$ and a unit value 1.0 for head scaling variable). Fixation-related SCD averaged for each condition was converted to a 2D space x 1D time image by flattening the sensor locations and interpolating the signals between them, where 32 pixels × 32 pixels represent the sensor-space data in the 2D space and 80-time points indicate 160 ms of 500 Hz sampling at 20–180 ms post-fixation. The images from the three task conditions were taken into a group level one-way ANOVA (within subjects) to identify the locations and time points that were significantly different among the conditions at an uncorrected $p < 0.001$ with a cluster extent threshold of at least 20 pixels (Fig. 3). The same analysis was applied separately for short and long saccades (Fig. 4).

2.6. Dynamic causal modeling (DCM)

DCM for event-related potential rests on a neural mass model to explain source activity, which incorporates the dynamics of three cortical layers: an excitatory subpopulation in the granular layer, an inhibitory subpopulation in the supra-granular layer and a subpopulation of deep pyramidal cells in the infra-granular layer (Jansen and Rit, 1995). Based on the extrinsic connectivity rules described by Felleman and Van Essen (1991), a number of cortical sources, each based on the neural mass model, are organized as a hierarchical cortico-cortical network. The strengths of extrinsic connections among the cortical sources are estimated using Variational Bayes (David et al., 2006). We applied this type of DCM to explain the generation of fixation-related evoked potentials of each task condition. All the DCM analysis steps were performed using SPM12 (Litvak et al., 2011).

First, to identify the cortical sources of interest, a source reconstruction method was applied to the FRP data (not to the SCDs). The anatomical MRI of each subject was segmented and spatially normalized to the Montreal Neurological Institute (MNI) space. EEG sensors were co-registered to the anatomical MRI and an individual forward head model was computed using a boundary element method (BEM). Based on a multiple sparse priors algorithm (Friston et al., 2008) that finds the optimal linear mixture of candidate priors (the source covariance matrix) to maximizes model evidence, a source 3D image of FRP for each subject was reconstructed for each of the task conditions and the fixation-cross condition. Band-pass filtered FRPs (0–250 Hz on the basis of Morlet wavelets) between 20 and 180 ms after fixation, which contains the main component of the activation (Fig. 2), were subjected to capture the whole evoked activity in the source level. A group level T-contrast was then computed for the three task images against the fixation-cross condition image with a threshold of $p < 0.005$ (uncorrected) and a cluster extent threshold of 100 voxels (Fig. 5A). Five MNI source coordinates were then identified based on the most significant increases in the source activations; these sources were located in the ventral visual pathway; bilateral V1 (−10, −96, −8; 22, −100, −8), bilateral V4 (−40, −88, −4; 48, −76, −2) and the right anterior inferotemporal area (IT; 48, −4, −42). The activation over the ventral visual cortex suggests that the presentation of scene images, as compared to the fixation-cross, has led the subject to identify and recognize the visual objects.

Given these prior source coordinates, six models of cortical structures were constructed with the driving input of the visual stimuli to V1 bilaterally (Fig. 5B). The models covered different levels of connections motivated by experimental studies of visual cortex (Felleman and Van Essen, 1991). Since we were interested in forward-backward complexity of the identified six regions (every region is connected), we confined the model space to the following six models. The simplest model 1 consists of only forward connections from bilateral V1 to ipsilateral V4 and from right V4 to right IT. Models 3 to 6 were based on model 1 with the difference that backward connections were added, namely between V4 and V1 with/without a connection from right IT to right V4. Lastly, lateral connections between left and right V4 were included in model 2, 4, and 6. Lateral connections between the sources of the second hierarchy were used in several DCM studies (e.g., David et al., 2006; Boly et al., 2011). FRPs over 0–200 ms post-fixation were fitted to the models. Activity of each cortical source was modeled with a single equivalent current dipole (ECD) method based on the individual forward head model (Kiebel et al., 2006). The effects of each task condition (free viewing, memorizing and searching) on the FRPs were contrasted against the fixation-cross condition, and modulatory effects on these contrasts were modeled for all extrinsic connections (i.e., between the sources) of the given model structure. In other words, the task-specific connectivity effects are relative to the "baseline-connectivity" of the fixation-cross condition. The same model space was also examined separately for short saccades and long saccades, where the effects of cognitive task conditions (memorizing, searching) were contrasted against the non-cognitive-task condition (free viewing) instead of the fixation-cross condition.

Bayesian model selection (BMS) was performed to identify the model structure within a confined model space that most likely generated the FRPs, assuming that – because of the basic nature of the tasks – that this model structure was the same for all subjects (i.e. a fixed-effects analysis was performed) (Stephan et al., 2010). The model evidence that accounts for both model accuracy and model complexity was used to determine posterior probabilities of the models (by normalizing the model evidence to the respective model space). Based on observed data, a large number of free parameters of the neural dynamics were estimated (Ostwald and

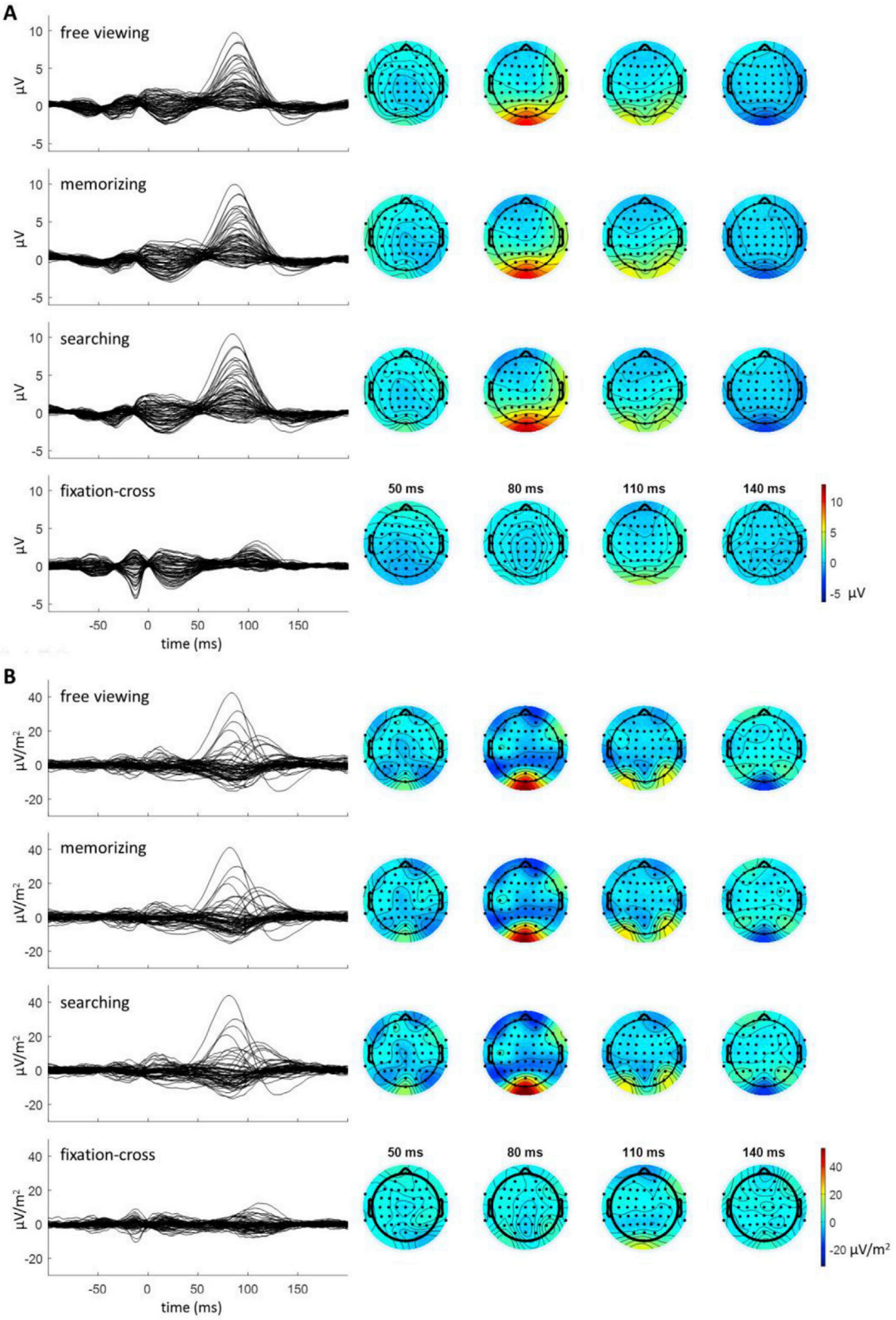

Fig. 2. Grand averaged fixation-related brain responses of event-related potential (A) and scalp current density (B). The left panels show individual electrode activities in a single plot for each condition and the right panels show the temporal courses of topographical maps. Note that scalp current density (SCD) reduces volume conduction effects by emphasizing sources at spatial scale over the surface.

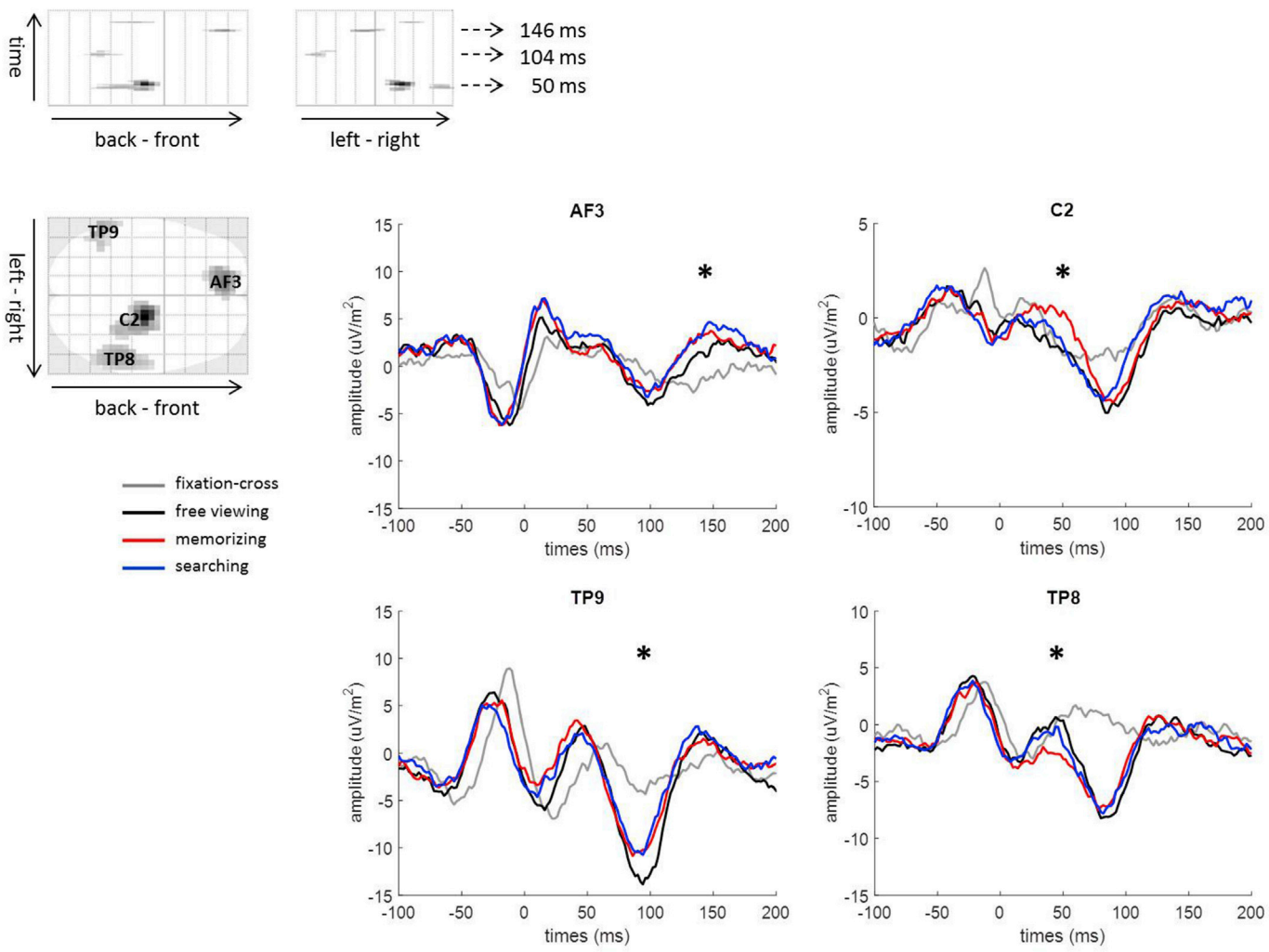

Fig. 3. Fixation-related scalp current density (SCD). Top left, significant main effect of task condition is shown in a 3D spatiotemporal map (20–180 ms post-fixation across all 63 electrodes) at a threshold of uncorrected $p < 0.001$ with an extent threshold of 20 pixels. Bottom right, SCD waveforms averaged by condition are shown for electrodes over the right frontal (AF3), bilateral temporal (TP8/9) and the right anterior parietal (C2) cortex, which electrodes showed the significant main effect of task condition. *, indicates the time phases when the significant main effect was found as shown on the top left. In cluster-level inference, AF3, TP8, TP9, and C2 showed p-values of 0.050, 0.007, 0.097, and 0.004, respectively. Only TP8 and C2 survived after cluster-level FWE correction ($p < 0.05$). Note that SCD responses during fixation-cross presentation (gray lines) were displayed for comparison purposes.

Starke, 2016). The extrinsic connectivity between cortical sources are commonly the most informative parameters that explain the changes in ERP data (David et al., 2006). From the winning model, the estimated modulatory connectivity parameters were subjected to a 2 (forward, backward) × 3 (free viewing, memorizing, searching) repeated measures ANOVA. The forward-backward asymmetry (direction index) was calculated by subtracting the sum of all backward connectivity estimates from the sum of all forward connectivity estimates.

3. Results

3.1. Task performance and eye-movement behavior

For searching, the subjects were able to find the location of the target object in about half of the thirty trials (mean 50.14% ± 3.63 SEM) with a mean response time of 3.05 s ± 0.07 SEM. For memorizing, individual mean accuracy in memorizing objects ranged from 30 to 66.67% (mean 48.08% ± 2.27 SEM), which is two times above the chance level of 20% (choosing one object from a set of five). These results support the assumption of cognitive engagement of the subjects during memorizing and searching conditions.

Fig. 1B–D shows the eye movement statistics in the three task conditions. Fixation durations (Fig. 1B) were longest when subjects freely viewed the scenes as compared to memorizing objects or searching a target object ($F_{2,50} = 15.010$, $p < 0.001$, $\varepsilon = 0.668$). Between memorizing and searching, there was no significant difference in fixation durations ($p = 0.789$). Saccade durations (Fig. 1C) were longer in the search condition, and shorter during the memorizing and free viewing condition ($F_{2,50} = 19.767$, $p < 0.001$, $\varepsilon = 0.742$). The differences between the search and the other conditions were significant (all corrected $p < 0.001$), while the difference between the memorizing and the free viewing conditions did not reach significance (Bonferroni corrected $p = 0.065$). Additionally, the histogram of saccade durations showed in all three task conditions a bimodal shape, indicating a separation between short and long saccades by about 26 ms (Fig. 1C). This suggests that the longer saccade durations during search was due to the increased proportion of long saccades, which is consistent with a recent study of eye movements in a visual search task (Nikolaev et al., 2016). Lastly, we observed a higher prevalence of horizontal over vertical saccade movements in all three task conditions (Fig. 1D), which is a typical characteristic for voluntary eye-movements (Nikolaev et al., 2016; Tatler and Vincent, 2008). Subjects also moved their eyes during fixation-cross presentations (fixation-cross condition)

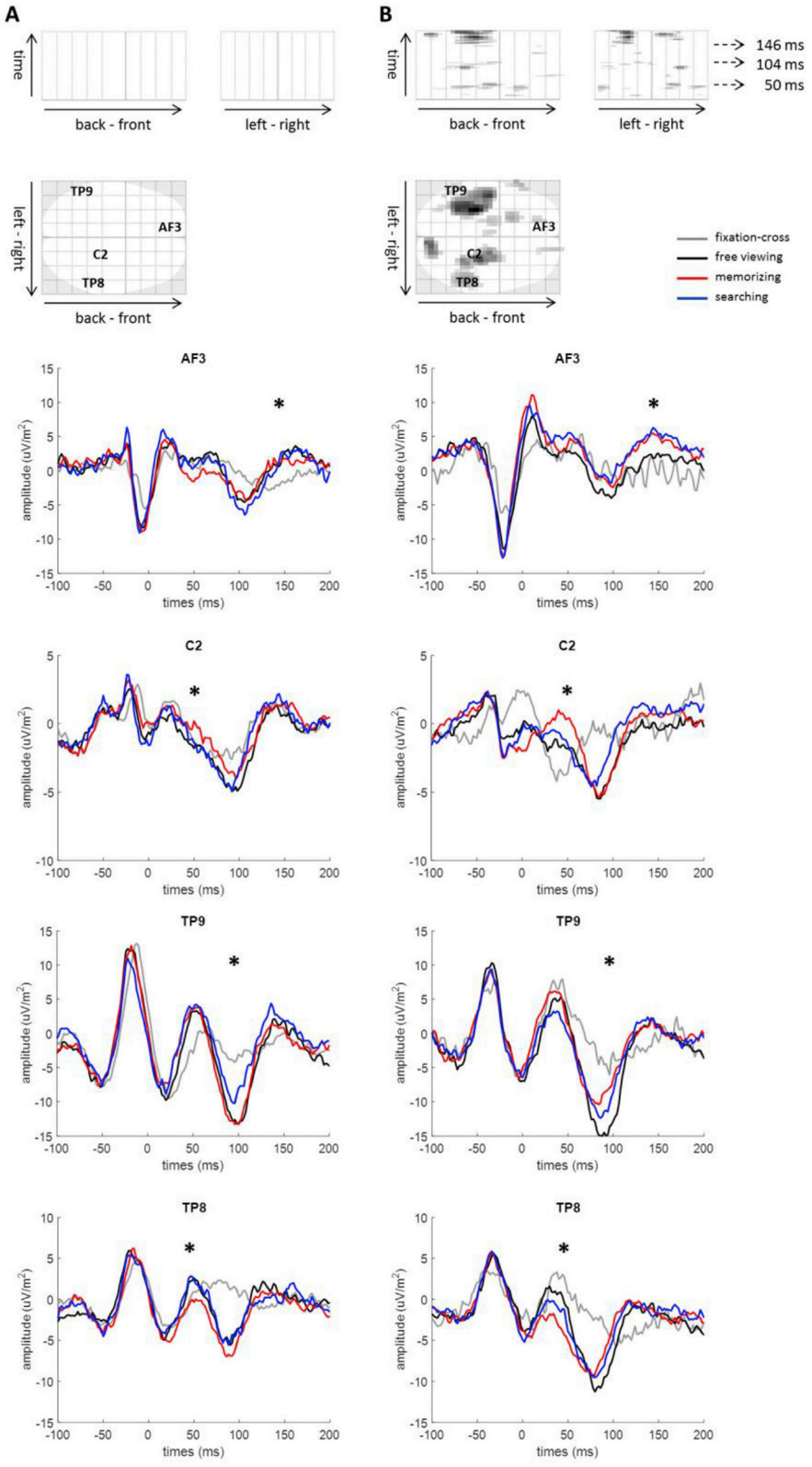

Fig. 4. Fixation-related scalp current density (SCD) for short saccades (A) and long saccades (B). The same test as in Fig. 3 was performed separately for short and long saccades. SCD waveforms averaged by condition are shown for electrodes such that revealed a significant main effect in Fig. 3.

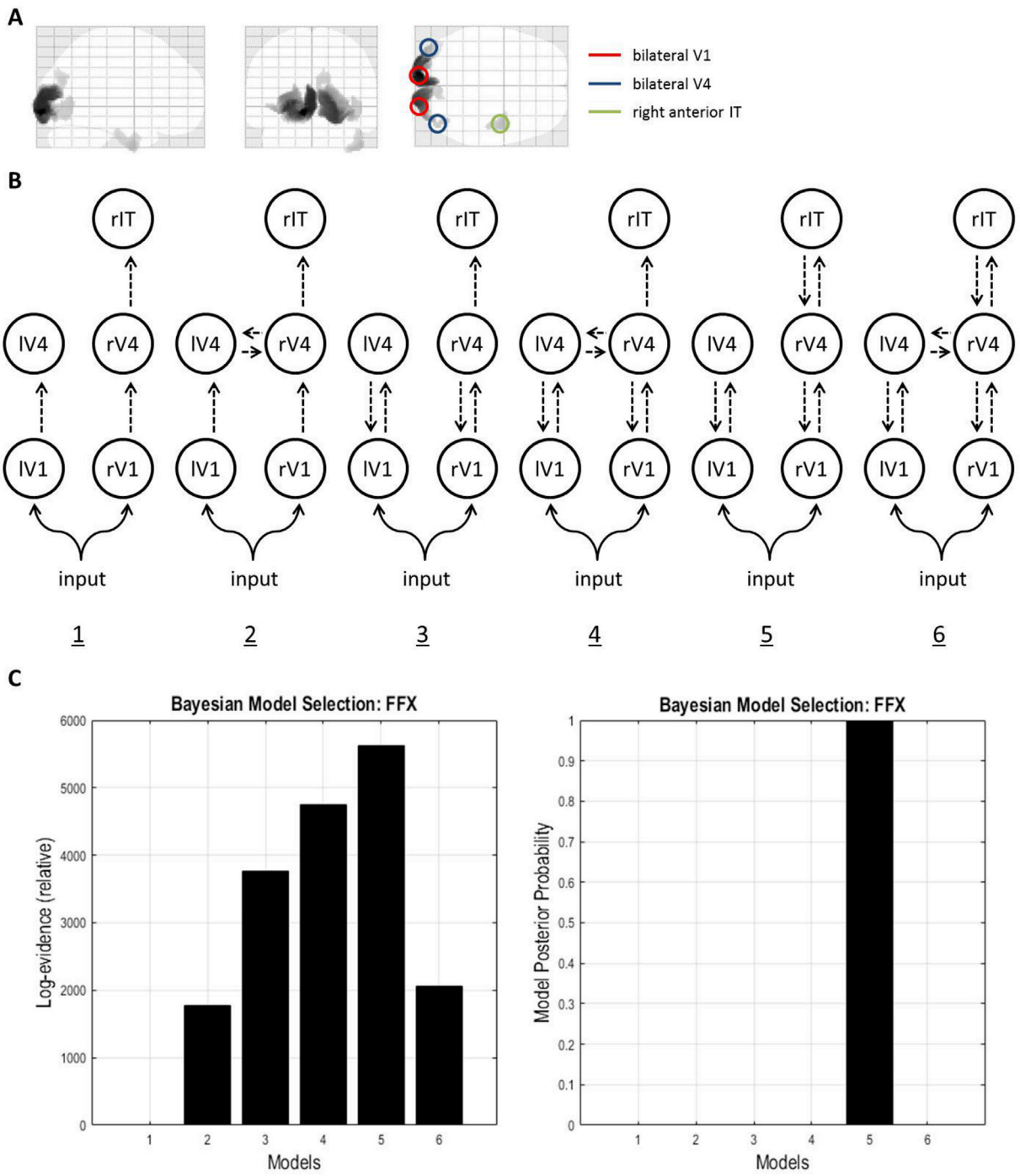

Fig. 5. DCM model space. (A) A distributed source reconstruction was performed on FRPs. The result of the T-contrast (task conditions vs. fixation-cross condition at 20–180 ms post-fixation) is shown at a threshold of uncorrected $p < 0.005$ with a cluster level of 100 voxels. Five MNI source coordinates were identified based on the most significant increases in power: the bilateral V1 (lV1: −10, −96, −8; rV1: 22, −100, −8), bilateral V4 (lV4: −40, −88, −4; rV4: 48, −76, −2) and the right anterior inferotemporal cortex (IT: 48, −4, −42). (B) Six model structures consist of a combination of forward, backward and bilateral connections among five brain regions identified above. (C) Results of the BMS analysis identified the best-fitting model 5 among all six competing candidates.

which were presented between task conditions (for details see Materials and Methods). Fixation durations were significantly longer than in the other three task conditions (284.12 ms ± 0.98 SEM; all corrected $p < 0.014$), while saccade durations were substantially shorter (15.92 ms ± 0.98 SEM; all corrected $p < 0.001$).

These findings indicate that the different task conditions had an influence on the features of the voluntary eye-movements, whereas the stimulus scene properties were kept comparable between task conditions. Therefore, we conclude that the condition-dependent changes of the eye-movements reflect different intentions of the subjects and are not due to stimulus-driven effects such as salient features.

3.2. Neural correlates of task conditions

The EEG activities during the tasks were first examined on the sensor space as fixation-related scalp current density (SCD; Kayser and Tenke, 2006), which highlights the local electrical activities and diminishes the volume conduction effects of EEG recordings. SCD estimates current

generators underlying the FRP, representing the magnitude of the radial current flow entering (positive) and leaving (negative) the scalp.

The occipital responses displayed characteristic components of the lambda wave (Fig. 2; Dimigen et al., 2009), consisting of three peaks; one central peak around Oz at about 80 ms and the other lateralized-peaks around PO7/8 at about 110 ms. It should be noted that the lateralized activity was not clearly recognized in the FRPs before SCD calculation. We also observed that the first activity at Oz was aligned more to saccade onset than to fixation onset, whereas the following lateralized activity was aligned more to fixation onset than to saccade onset (Supplementary Fig. 2).

Fig. 3 illustrates the differences in the fixation-related SCDs between three task conditions. Significant task effects were found over the right hemisphere covering the temporal cortex (TP8) and the anterior parietal cortex (C2). The largest positive SCD was found during memorizing followed by searching and free viewing at C2 around 50 ms after fixation onset. In contrast, toward a negative value was found during memorizing at TP8 electrode. These results suggest differential involvement of cortical responses between task conditions, namely that cortical areas responded in different ways when different cognitive tasks were required (see also the Supplementary Fig. 3 for FRPs).

Because the saccade durations varied between the task conditions, it could be argued that the task-dependent cortical responses might be due to the different saccade durations rather than reflecting task-dependent cognitive processes. To test this possibility, short saccades ($\leq$26 ms) and long saccades (>26 ms) were analyzed separately. We obtained a similar pattern of results to the main findings over the four cortical regions defined above, especially during the long saccadic movements (Fig. 4). It should also be noted that the baseline activity from −100 to 0 ms before fixation onset, which might reflect the difference in saccade durations, showed qualitatively similar waveforms in the three task conditions than the task-dependent cortical responses. Therefore, the task-dependent changes in fixation-related SCDs were less likely to be attributed to the difference in saccade durations.

3.3. Task-dependent forward-backward cortical loops

If the observed differences in the evoked response pattern is the result of different top-down cognitive mechanisms and evoked response is generated by forward and backward loops in cortical networks (Garrido et al., 2007), task-dependent modulations of forward and backward functional connections can be predicted. To test this question, we employed DCM to infer functional connection strengths among cortical regions and their modulations between task conditions (David et al., 2006). The cortical regions for DCM analysis were extracted based on a source reconstruction of the FRPs. The comparison of the source images obtained from the three task conditions to the source images obtained from the fixation-cross condition led to the conclusion that the strongest differences were found over the ventral visual pathway (Fig. 5A). The source activities with significant differences between the task conditions and the fixation-cross condition were located in the following five Montreal Neurological Institute (MNI) source coordinates: bilateral V1 (−10, −96, −8; 22, −100, −8), bilateral V4 (−40, −88, −4; 48, −76, −2) and right anterior inferotemporal cortex (IT; 48, −4, −42). We adopted these sources as the nodes of the cortical network for DCM analysis. Subsequently, we constructed six different models (Fig. 5B) on the basis of previous findings about structural and functional connectivity in the visual cortex (Felleman and Van Essen, 1991), which cover the bilateral, forward and backward connections among these cortical regions. The DCM modulatory effects of the three task conditions were then estimated in contrast to the fixation-cross condition for each of these six models. The result of the Bayesian model selection (BMS; Stephan et al., 2010) revealed that model 5 best explained the observed data (Fig. 5C and Supplementary Fig. 4).

Fig. 6 shows the modulations of functional connectivity in model 5 for each task condition. The modulatory effects of forward and backward connections were examined for each connection, i.e., between lV1 and lV4, between rV1 and rV4, and between rV4 and rIT. Two-way repeated measures ANOVAs were applied with the factors *direction* (forward and backward) and *condition* (free viewing, memorizing and searching) and we found a significant main effect of *direction* between lV1 and lV4 ($F_{1,25} = 14.047$, $p = 0.001$; Fig. 6A). Also, we found a significant interaction effect of *direction* × *condition* between rV1 and rV4 ($F_{2,50} = 5.805$, $p = 0.005$). A similar pattern of modulations was observed between rV4 and rIT (i.e., the interaction between memorizing and searching), however, it did not reveal a significant interaction effect ($F_{1.41,35.35} = 1.753$, $p = 0.194$). No other significant main or interaction effect was observed (all $p > 0.531$). The significant effects suggested the forward-backward asymmetry of the connectivity strengths and its task-dependent modulation.

To assess the overall modulatory effects over the ventral visual pathway, and in particular the bottom up and top down components, we compared the sum of the forward (Fig. 6B) as well as the backward (Fig. 6C) functional connectivity strengths across connections using the same 2 × 3 repeated measures ANOVA. This comparison discovered a significant main effect of *direction* ($F_{1,25} = 5.752$, $p = 0.024$), indicating that the task conditions, relative to fixation-cross condition, overall induced a stronger forward (mean 0.243 ± 0.153 SEM; Fig. 6B) than backward connections (mean -0.008 ± 0.133 SEM; Fig. 6C). In addition, the sum of the forward connections was significantly above zero in the memorizing task (mean 0.464 ± 0.171 SEM, $p = 0.012$; Fig. 6B), but did not reach significance during the free viewing (mean 0.236 ± 0.176 SEM, $p = 0.193$) and searching (mean 0.029 ± 0.182 SEM, $p = 0.873$) tasks. Of interest, it revealed a significant interaction effect of *direction* × *condition* ($F_{1,50} = 6.339$, $p = 0.004$), indicating a task-dependent forward-backward functional connectivity. To study this further, we defined a *direction index*, which quantifies the forward-backward asymmetry of the connectivity, by subtracting the sum of all backward connectivity strengths from the sum of all forward connectivity strengths. Based on the comparison of these measures from the different task conditions (using paired t-tests) we found a significant enhancement towards backward connectivity during the search task as compared to the memorizing, whereas the memorizing task showed an enhanced forward connectivity (Bonferroni corrected $p < 0.001$; Fig. 6D). For the other pairwise comparisons of the task conditions we did not find a significant difference (Bonferroni corrected $p > 0.189$).

A potential influence of saccade durations on DCM results was additionally examined by using the same model space (Fig. 5B), however, separately for short ($\leq$26 ms) or long (>26 ms) saccades. Since saccades during the fixation-cross condition were mainly constituted by short saccades (Fig. 1C), FRPs were examined on cognitive-task conditions (memorizing and searching) in contrast to the non-cognitive-task condition (free viewing). This also ensured that presentations of visual stimulus were comparable between conditions. Fig. 7A and B shows that model 5 was significantly more favorable than the other models in both short and long saccades, confirming the significant involvement of forward and backward connections in the generation of FRPs when high cognitive demands were required. The functional connection strengths revealed a significant *direction* × *condition* effect between rV1 and rV4 ($F_{1,25} = 4.395$, $p = 0.046$) and reduced direction index during searching as compared to memorizing (one-tailed paired *t*-test $p = 0.029$), which are in line with the results above (Fig. 6). In contrast, for short saccades, we observed no significant main or interaction effect (all $p > 0.237$; Fig. 7C). In both saccades, we found no *direction* effect in any connection (all $p > 0.218$), suggesting the absence of a stronger forward connection when the model estimation was performed on conditions that have comparable visual properties (i.e., memorizing, searching vs. free viewing).

4. Discussion

In the present study we investigated the fixation-related evoked

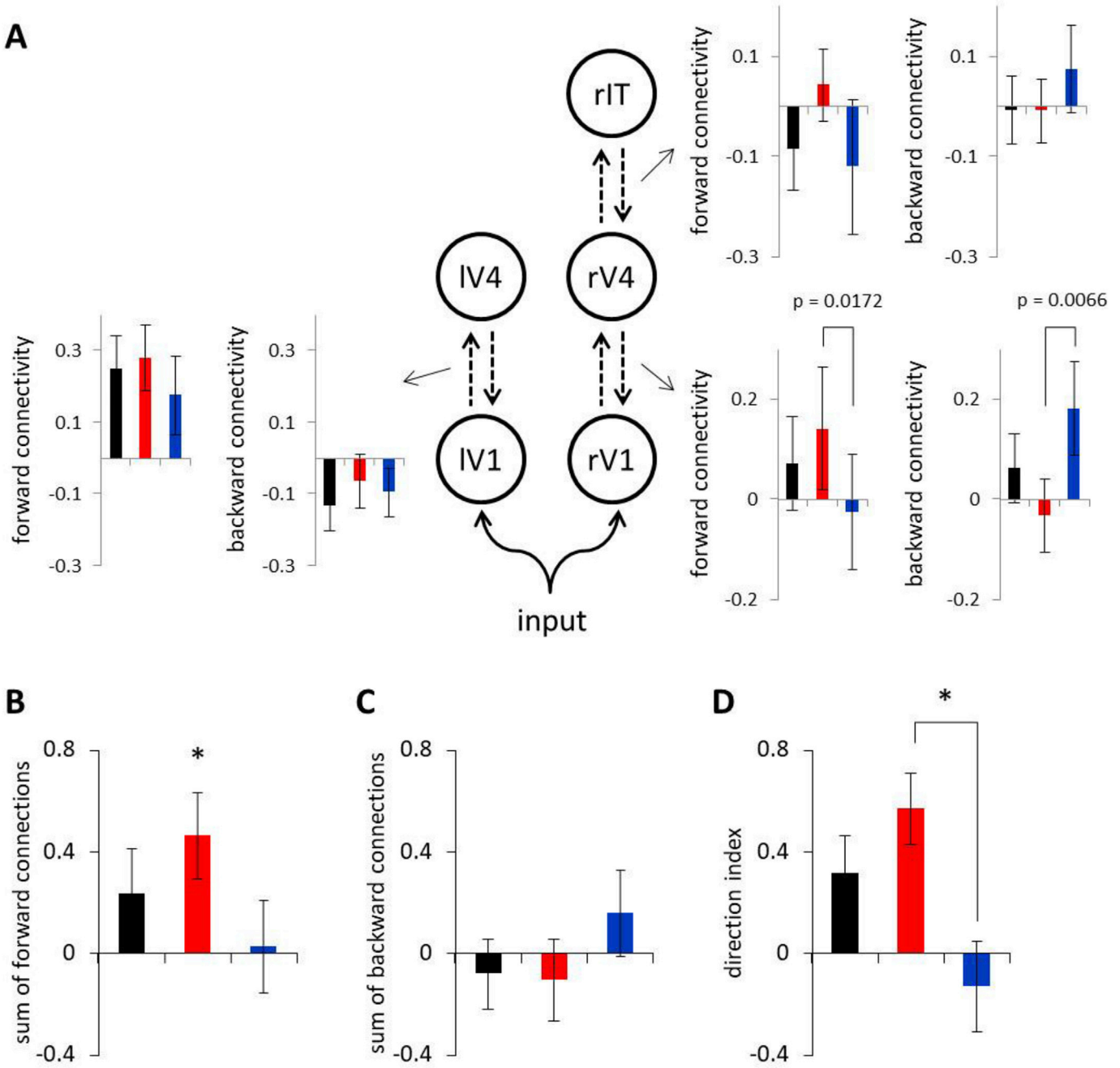

Fig. 6. Functional connectivity strengths of model 5. (A), Forward and backward connectivity strengths are shown for each connection and significant differences in functional connectivity between conditions are indicated by p-values (two-tailed paired *t*-test, uncorrected $p < 0.05$). The sums of all forward and backward connections are shown in (B) and (C), respectively. (D) The direction index is the difference between the sum of all forward and backward connections (forward – backward connections). A more negative value indicates more strengthened backward connections relative to forward connections. A significant difference in the direction index was found between memorizing and searching (two-tailed paired *t*-test, uncorrected $p = 0.0002$). Error bars represent standard error of the mean. *, $p < 0.05$.

responses under three different task conditions, i.e., memorizing, searching and free viewing of complex visual objects in natural scenes. We found task-dependent differences in the fixation-related SCDs at TP8 and C2 electrodes. Source reconstruction of the FRPs suggested that these differences reflected task-dependent modulations of source activities in the ventral visual pathway, specifically, bilateral V1, bilateral V4 and right IT. DCM analysis based on these source activities revealed that the strength of hierarchical forward-backward functional connections between these sources was modulated depending on the cognitive task: memorizing objects enhanced the asymmetry toward forward connections, whereas searching a target object enhanced backward connections. In the following we discuss physiological and functional implications of these results from various aspects.

4.1. Neural correlates of visual information processing

FRPs displayed characteristic components of the lambda wave around 100 ms after fixation onset. In agreement with the literature (e.g., Ossandón et al., 2010), the lambda wave was best elicited over the occipital region when a complex image was presented as compared to the presentation of non-visual information (the fixation-cross condition). Notably, in the present study, spatial and temporal separation of

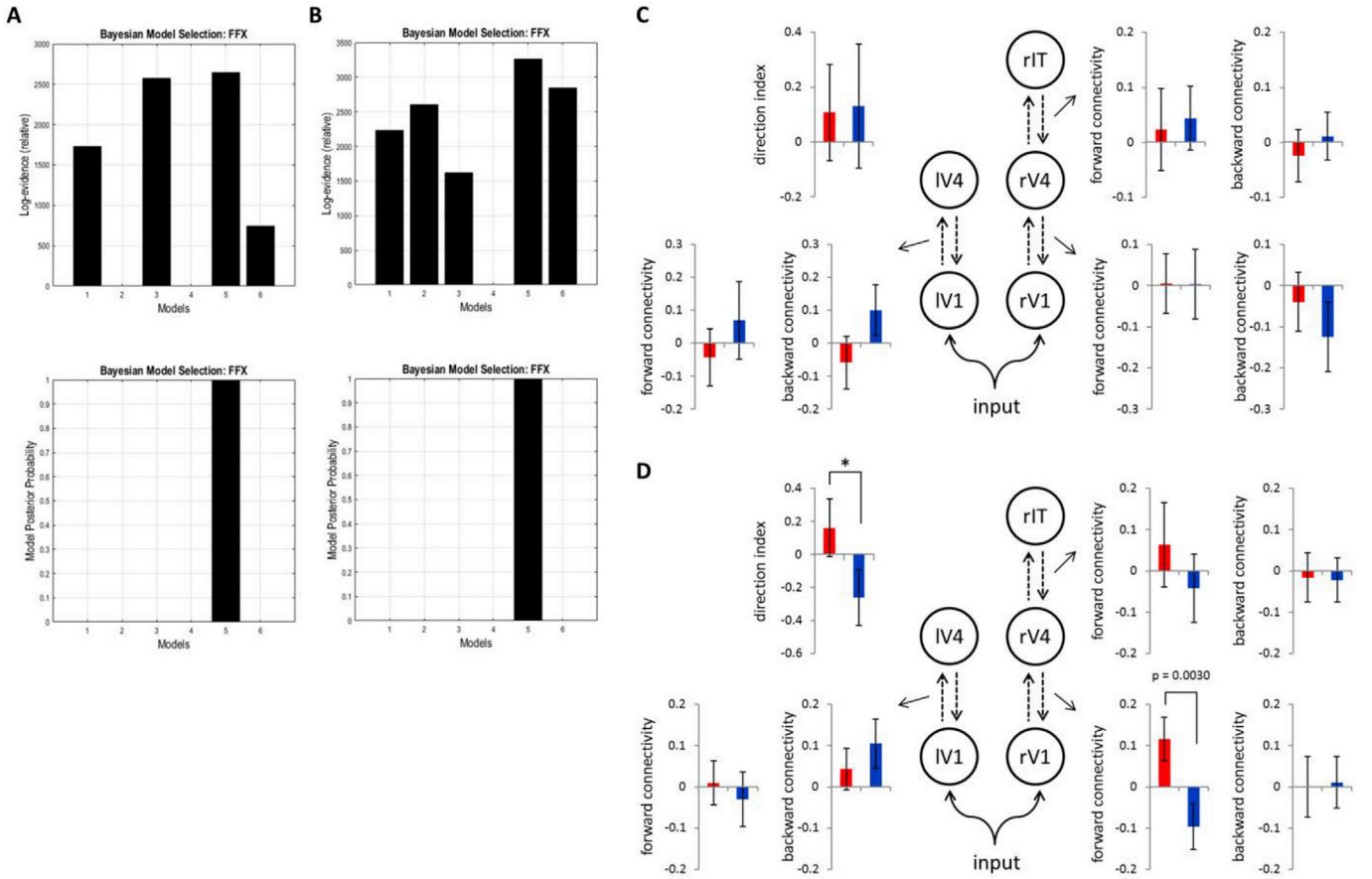

Fig. 7. Model estimates of short saccades and long saccades. The model space in Fig. 5B was examined for short (A) and long (B) saccade FRPs in which FRPs during memorizing and searching were contrasted against the non-cognitive-task condition (i.e., free viewing). Both BMS results revealed that model 5 is significantly favorable than its counterparts (A, B). Functional connectivity strengths of model 5 for short (C) and long saccades (D) are shown. Significant differences (one-tailed paired *t*-test, uncorrected $p < 0.05$) in forward and backward connectivities between conditions are indicated by p-values. The direction index is the difference between the sum of all forward and backward connections (forward – backward connections). A more negative value indicates more strengthened backward connections relative to forward connections. The direction index shows significant effect on long saccades (one-tailed paired *t*-test, $p = 0.029$; indicated by an asterisk in D). Red and blue bars indicate memorizing and searching, respectively. Error bars represent standard error of the mean.

components could be established: one peak at Oz, which was time-locked to saccade onset, and the other peaks at PO7/8, locked to fixation onset (Supplementary Fig. 2). This separation became markedly visible after SCD calculation. This result is supported by the hypothesis that the lambda wave is a compound of activity evoked by both saccade and fixation onsets (for a review, see Nikolaev et al., 2016). Since complex object representations are formed in the higher-order areas (V4, IT) that lie lateral to V1 (Kravitz et al., 2013), we speculate that the lateralized activity resulted from fixation onset would reflect the recognition process of complex objects.

Furthermore, our cortical source reconstruction localized the activity in the ventral visual cortex, which constitutes neural representations of the visual properties of an object (Goodale and Milner, 1992). In contrast, however, during fixation-cross condition the activity over V1 was reduced with a longer latency of 110 ms and the lateralized-peaks were absent. These results confirmed that the evoked responses are associated with visual information processing and the observed activity in the ventral visual cortex could associate with object-identification and/or object-recognition during processing of the complex scene images (it is not necessarily restricted to the embedded objects but also to other objects that were already part of the complex scene).

4.2. Neural correlates of top-down processing

Current visual processing theory suggested that top-down signaling facilitate neurons to transfer task-relevant information (Gilbert and Li, 2013). We found the changes in cortical responses depending on different task conditions during which the same visual features were presented. This suggested that, instead of a mere bottom-up effect, endogenous top-down processing caused task-dependent modulations of cortical responses over different areas in different time periods, indicating distinct signal processing throughout the cortical regions for different conditions. However, although the SCDs revealed significant task effect, the effect should not be over-interpreted and additional studies are required to validate the modest effect on FRPs.

Visually evoked electrical and magnetic responses have been identified at the earliest of 50 ms post-stimulus of visual control (Jeffreys, 1971; Clark et al., 1995; Poghosyan and Ioannides, 2008). Although some studies argue that top-down control on the visual information process occurs later in time (for a review see Theeuwes, 2010), several recent studies associates the early visual response with top-down effects (for a review see Rauss et al., 2011). The present results of the fixation-related SCDs with the earliest task effect at about 50 ms suggest that top-down processing rendered cortical responses modifiable according to cognitive demands very early during visual processing.

4.3. Task-dependent forward-backward cortical loops

The model that was best supported by the data (in terms of model-evidence) of the observed FRPs showed that task-dependent visual

processing rests on the modulation of forward and backward connections. The observation of increased forward connectivity during the task conditions (vs. fixation-cross condition) could have facilitated information processing of the salient visual features embedded in a complex scene image (Lamme and Roelfsema, 2000). Hence, the connectivity strength biased toward forward connections may allow efficient processing of the visual inputs. Memorizing objects might be subjected to enhanced forward connections since incoming visual properties need to be encoded into memory in addition to mere processing. Accordingly, we found enhanced forward over backward connectivities during memorizing which were more pronounced than other task conditions. This finding points to a significant role of the forward pathway during memorizing and that neurons carry more information about the attended visual features of the lower-order areas (Gazzaley and Nobre, 2012; Li et al., 2004). The enhanced forward connections in the present study might have promoted encoding of visual features into memory.

In contrast to memorizing objects, searching a target object essentially rests on prior information about visual features of the target. During searching, the asymmetry toward backward connections was higher than that elicited by the memorizing condition. This result suggests that during searching a target object, visual processing could be guided by higher-level areas through backward connections providing top-down control (Gilbert and Li, 2013). This view is in accordance with the behavioral finding that searching a target object is primarily associated with cognitive top-down control on the salience effect, i.e., stimulus-driven bottom-up guidance (Bacon and Egeth, 1994; Chen and Zelinsky, 2008; Wolfe et al., 2003). We therefore suggest that backward connections from higher-level to lower-level cortical areas offer a possible mechanism by which prior information might be used in order to guide visual search.

4.4. Limitations and future studies

In this study we opted for a rather scarce model space because we were interested in general asymmetry between forward and backward connectivities and their modulations. As a consequence, we confined the model space according to our research question and did not test all possible connectivity architectures. We believe that future studies could build on our findings and thus will help to establish the complete network underpinning the functional organization of top-down visual processing.

Second, the presentation of fixation-cross might be not an ideal reference for contrasting three task conditions in DCM, since the visual stimuli were physically not identical. With this account, the finding of Fig. 6 should be interpreted with caution, because stimulus-specific activity might confound the effect. Notably, this finding was consistent with the following DCM results, where the free viewing condition was contrasted with the other two task conditions, ensuring no significant difference in stimulus presentations (Fig. 7). Therefore, especially during long saccadic movement, the consistent results of model selection and the task effect of forward-backward asymmetry were not likely due to the stimulus-specific activity, but rather to a difference of cognitive process.

Third, task effects on cortical responses were observed particularly for long saccades when saccadic movements were split into short and long durations. Hence, on the basis of the present results, it seems plausible that the change of cognitive processing prevailed during long saccadic movements. However, since visual properties presented on the screen and the task goals could result in a complex scanning strategy, we cannot conclude that the cognitive task effects are solely attributed to long saccadic movements. For instance, during the cognitive-task conditions (memorizing and searching), the eye-movement behavior reflects the likelihood of making long saccades together with short fixations. In previous studies (e.g., Ito et al., 2017; Unema et al., 2005), this phenomenon has been mainly reported for the early viewing phase of scene perception (global scanning) under free viewing conditions, whereas, in a later phase, the behavior usually shifts into short saccades (local scanning). Therefore, if saccade and fixation activities are governed by a common mechanism (Unema et al., 2005), cognitive task conditions might render a different sequence of eye-movements, retaining global scanning.

Lastly, visual selective attention to global and local processing is suggested to play a role in the hemispheric asymmetry (Hellige, 1996; Robertson and Lamb, 1991); the right and left hemispheres are associated with encoding global and local visual features, respectively. Indeed, in the cortical sensor level, we observed differential hemispheric asymmetry between task conditions covering the temporal and parietal lobes. Therefore, the aspects of visual attention might have involved differently between task conditions. However, it should be noted that because the designation of the memorizing and searching conditions made subjects consciously identifying objects on complex scene images, it is presumed that visual attention directed to the objects was similarly allocated between the memorizing and searching conditions. Disentangling the respective contributions of the two eye-movement behaviors (global and local scanning) in relation to cortical responses would help to address this question of the hemispheric asymmetry underlying the high-demanding cognitive processing.

5. Conclusion

We investigated the generative model of fixation evoked responses to each task condition. We found characteristic components of the lambda wave when a scene image was presented, which are most likely generated by forward-backward cortical loops in the ventral visual cortex. Further, a greater modulatory effect on the hierarchical forward-backward asymmetry was found during cognitive task conditions relative to the condition where no specific task was required; memorizing objects enhanced the asymmetry toward forward connections, whereas searching a target object enhanced the backward connections. Future studies need to determine whether the hierarchical forward-backward asymmetry also mediates other sensory processes, which will elucidate a general principle of top-down influences on sensory processing and perception.

Acknowledgements

This work was supported by the International Research Training Group (IRTG 2150) of the German Research Foundation (DFG), the European Union's Horizon 2020 research and innovation programme under grant agreement No. 720270 (HBP), and START-Program of the Faculty of Medicine, RWTH Aachen (START 135/14).

Appendix A. Supplementary data

Supplementary data to this article can be found online at https://doi.org/10.1016/j.neuroimage.2019.02.068.

Conflicts of interest

The authors declare no competing interests.

References

Allen, P.J., Polizzi, G., Krakow, K., Fish, D.R., Lemieux, L., 1998. Identification of EEG events in the MR scanner: the problem of pulse artifact and a method for its subtraction. Neuroimage 8 (3), 229–239.
Allen, P.J., Josephs, O., Turner, R., 2000. A method for removing imaging artifact from continuous EEG recorded during functional MRI. Neuroimage 12 (2), 230–239.
Bacon, W.F., Egeth, H.E., 1994. Overriding stimulus-driven attentional capture. Percept. Psychophys. 55 (5), 485–496.
Boly, M., Garrido, M.I., Gosseries, O., Bruno, M.A., Boveroux, P., Schnakers, C., Massimini, M., Litvak, V., Laureys, S., Friston, K., 2011. Preserved feedforward but impaired top-down processes in the vegetative state. Science 332, 858–862.
Chen, X., Zelinsky, G.J., 2008. Real-world visual search is dominated by top-down guidance. Vis. Res. 46 (24), 4118–4133.

Clark, V.P., Fan, S., Hillyard, S.A., 1995. Identification of early visual evoked potential generators by retinotopic and topographic analyses. Hum. Brain Mapp. 2, 170–187.
David, O., Kiebel, S.J., Harrison, L.M., Mattout, J., Kilner, J.M., Friston, K.J., 2006. Dynamic causal modeling of evoked responses in EEG and MEG. Neuroimage 30 (4), 1255–1272.
Delorme, A., Makeig, S., 2004. EEGLAB: an open source toolbox for analysis of single-trial EEG dynamics including independent component analysis. J. Neurosci. Methods 134 (1), 9–21.
Dimigen, O., Valsecchi, M., Sommer, W., Kliegl, R., 2009. Human microsaccade-related visual brain responses. J. Neurosci. 29 (39), 12321–12331.
Dimigen, O., Sommer, W., Hohlfeld, A., Jacobs, A.M., Kliegl, R., 2011. Coregistration of eye movements and EEG in natural reading: analyses and review. J. Exp. Psychol. Gen. 140 (4), 552–572.
Engbert, R., Mergenthaler, K., 2006. Microsaccades are triggered by low retinal image slip. Proc. Natl. Acad. Sci. U.S.A. 103 (18), 7192–7197.
Felleman, D.J., Van Essen, D.C., 1991. Distributed hierarchical processing in the primate cerebral cortex. Cerebr. Cortex 1 (1), 1–47.
Friston, K., Harrison, L., Daunizeau, J., Kiebel, S., Phillips, C., Trujillo-Barreto, N., Henson, R., Flandin, G., Mattout, J., 2008. Multiple sparse priors for the M/EEG inverse problem. Neuroimage 39, 1104–1120.
Garrido, M.I., Kilner, J.M., Kiebel, S.J., Friston, K.J., 2007. Evoked brain responses are generated by feedback loops. Proc. Natl. Acad. Sci. U.S.A. 104 (52), 20961–20966.
Gazzaley, A., Nobre, A.C., 2012. Top-down modulation: bridging selective attention and working memory. Trends Cognit. Sci. 16 (2), 129–135.
Gilbert, C.D., Li, W., 2013. Top-down influences on visual processing. Nat. Rev. Neurosci. 14, 350–363.
Goodale, M., Milner, A., 1992. Separate visual pathways for perception and action. Trends Neurosci. 15 (1), 20–25.
Hellige, J.B., 1996. Hemispheric asymmetry for visual information processing. Acta Neurobiol. Exp. 56 (1), 485–497.
Ito, J., Yamane, Y., Suzuki, M., Maldonado, P., Fujita, I., Tamura, H., Grün, S., 2017. Switch from ambient to focal processing mode explains the dynamics of free viewing eye movements. Sci. Rep. 7 (1), 1082.
Jansen, B.H., Rit, V.G., 1995. Electroencephalogram and visual evoked potential generation in a mathematical model of coupled cortical columns. Biol. Cybern. 73, 357–366.
Jeffreys, D.A., 1971. Cortical source locations of pattern-related visual evoked potentials recorded from the human scalp. Nature 229, 502–504.
Kamienkowski, J.E., Ison, M.J., Quiroga, R.Q., Sigman, M., 2012. Fixation-related potentials in visual search: a combined EEG and eye tracking study. J. Vis. 12 (7), 4.
Kaunitz, L.N., Kamienkowski, J.E., Varatharajah, A., Sigman, M., Quiroga, R.Q., Ison, M.J., 2014. Looking for a face in the crowd: fixation-related potentials in an eye-movement visual search task. Neuroimage 89, 297–305.
Kayser, J., Tenke, C.E., 2006. Principal components analysis of Laplacian waveforms as a generic method for identifying ERP generator patterns: I. Evaluation with auditory oddball tasks. Clin. Neurophysiol. 117 (2), 348–368.
Kiebel, S.J., David, O., Friston, K.J., 2006. Dynamic causal modelling of evoked responses in EEG/MEG with lead field parameterization. Neuroimage 30 (4), 1273–1284.
Kravitz, D.J., Saleem, K.S., Baker, C.I., Ungerleider, L.G., Mishkin, M., 2013. The ventral visual pathway: an expanded neural framework for the processing of object quality. Trends Cognit. Sci. 17 (1), 26–49.
Lamme, V.A., Roelfsema, P.R., 2000. The distinct modes of vision offered by feedforward and recurrent processing. Trends Neurosci. 23 (11), 571–579.
Li, W., Piëch, V., Gilbert, C.D., 2004. Perceptual learning and top-down influences in primary visual cortex. Nat. Neurosci. 7, 651–657.
Litvak, V., Mattout, J., Kiebel, S., Phillips, C., Henson, R., Kilner, J., Barnes, G., Oostenveld, R., Daunizeau, J., Flandin, G., Penny, W., Friston, K., 2011. EEG and MEG data analysis in SPM8. Comput. Intell. Neurosci. 2011, 852961.
Nikolaev, A.R., Meghanathan, R.N., van Leeuwen, C., 2016. Combining EEG and eye movement recording in free viewing: pitfalls and possibilities. Brain Cogn. 107, 55–83.
Oldfield, R.C., 1971. The assessment and analysis of handedness: the Edinburgh inventory. Neuropsychologia 9 (1), 97–113.
Ossandón, J.P., Helo, A.V., Montefusco-Siegmund, R., Maldonado, P.E., 2010. Superposition model predicts EEG occipital activity during free viewing of natural scenes. J. Neurosci. 30 (13), 4787–4795.
Ostwald, D., Starke, L., 2016. Probabilistic delay differential equation modeling of event-related potentials. Neuroimage 136, 227–257.
Poghosyan, V., Ioannides, A.A., 2008. Attention modulates earliest responses in the primary auditory and visual cortices. Neuron 58 (6), 802–813.
Pollen, D.A., 1999. On the neural correlates of visual perception. Cerebr. Cortex 9 (1), 4–19.
Rauss, K., Schwartz, S., Pourtois, G., 2011. Top-down effects on early visual processing in humans: a predictive coding framework. Neurosci. Biobehav. Rev. 35, 1237–1253.
Robertson, L.C., Lamb, M.R., 1991. Neuropsychological contributions to theories of part/whole organization. Cogn. Psychol. 23 (2), 299–330.
Stephan, K.E., Penny, W.D., Moran, R.J., den Ouden, H.E., Daunizeau, J., Friston, K.J., 2010. Ten simple rules for dynamic causal modeling. Neuroimage 49 (4), 3099–3109.
Tatler, B.W., Vincent, B.T., 2008. Systematic tendencies in scene viewing. J. Eye Mov. Res. 2 (2), 5.
Theeuwes, J., 2010. Top-down and bottom-up control of visual selection. Acta Psychol. 135, 77–99.
Unema, P.J., Pannasch, S., Joos, M., Velichkovsky, B.M., 2005. Time course of information processing during scene perception: the relationship between saccade amplitude and fixation duration. Vis. Cognit. 12, 473–494.
Wolfe, J.M., Butcher, S.J., Lee, C., Hyle, M., 2003. Changing your mind: on the contributions of top-down and bottom-up guidance in visual search for feature singletons. J. Exp. Psychol. Hum. Percept. Perform. 29 (2), 483–502.